



Title	MDM2 regulates a novel form of incomplete neoplastic transformation of Theileria parva infected lymphocytes
Author(s)	Hayashida, Kyoko; Kajino, Kiichi; Hattori, Masakazu; Wallace, Maura; Morrison, Ivan; Greene, Mark I.; Sugimoto, Chihiro
Citation	Experimental and Molecular Pathology, 94(1), 228-238 https://doi.org/10.1016/j.yexmp.2012.08.008
Issue Date	2013-02
Doc URL	http://hdl.handle.net/2115/52236
Type	article (author version)
File Information	EMP94-1_228-238.pdf



[Instructions for use](#)

MDM2 regulates a novel form of incomplete neoplastic transformation of *Theileria parva* infected lymphocytes

**Kyoko Hayashida¹, Kiichi Kajino¹, Masakazu Hattori², Maura Wallace³, Ivan Morrison⁴,
Mark I. Greene⁵, and Chihiro Sugimoto¹**

¹From the Division of Collaboration and Education, Hokkaido University

Research Center for Zoonosis Control, Sapporo 001-0020, Japan

²Center for Innovation in Immunoregulative Technology and Therapeutics, Graduate School of Medicine, Kyoto

University, Kyoto, Japan

³Department of Veterinary Clinical Studies, University of Edinburgh, Easter Bush Veterinary Centre, Roslin,

Midlothian EH25 9RG, United Kingdom

⁴The Roslin Institute, Royal (Dick) School of Veterinary Studies, University of Edinburgh, Easter Bush, Roslin,

Midlothian EH25 9RG, United Kingdom

⁵Department of Pathology and Laboratory Medicine, University of Pennsylvania, Philadelphia, PA 19104-6082,

USA

Running title: MDM2 dependent transformation of *T. parva* infected lymphocyte

To whom correspondence should be addressed: Chihiro Sugimoto, Division of Collaboration and Education, Hokkaido University Research Center for Zoonosis Control, Sapporo 001-0020, Hokkaido, Japan. Tel.: (81) 11-706-5297; Fax: (81) 11-706-7370; E-mail: sugimoto@czc.hokudai.ac.jp

Keywords: Lymphoproliferation; *Theileria parva*; MDM2; p53

ABSTRACT

Our efforts are concerned with identifying features of incomplete malignant transformation caused by non viral pathogens. *Theileria parva* (*T. parva*) is a tick-transmitted protozoan parasite that can cause a fatal lymphoproliferative disease in cattle. The *T. parva*-infected lymphocytes display a transformed phenotype and proliferate in culture media like the other tumor cells, however those cells will return to normal after antiprotozoal treatment reflecting the incomplete nature of transformation. To identify signaling pathways involved in this form of transformation of *T. parva*-infected cells, we screened a library of anticancer compounds. Among these, TIBC, a specific inhibitor of MDM2, markedly inhibited proliferation of *T. parva*-infected

lymphocytes and promoted apoptosis. Therefore we analyzed MDM2 function in *T. parva*-infected cells. Several *T. parva*-infected cell lines showed increased expression level of MDM2 with alternatively spliced isoforms compared to the lymphoma cells or ConA blasts. In addition, buparvaquone affected MDM2 expression in *T. parva* transformed cells. Moreover, p53 protein accumulation and function were impaired in *T. parva*-infected cells after cisplatin induced DNA damage despite the increased p53 transcription level. Finally, the treatment of *T. parva*-infected cells with boronic-chalcone derivatives TIBC restored p53 protein accumulation and induced Bax expression. These results suggest that the overexpression of MDM2 is closely linked to the inhibition of p53-dependent apoptosis of *T. parva*-infected lymphocytes. Aberrant expression of host lymphocyte MDM2 induced by cytoplasmic existence of *T. parva*, directly and/or indirectly, is associated with aspects of this type of transformation of *T. parva*-infected lymphocytes. This form of transformation shares features of oncogene induced malignant phenotype acquisition.

Introduction

Members of the genus *Theileria* are intracellular apicomplexan protozoan parasites transmitted by ticks. Among several *Theileria* species, *T. parva* is highly pathogenic for cattle and cause fatal lymphoproliferative diseases known as East Coast fever (Brown et al., 1973; Irvin et al., 1975; Lawrence and Irvin, 1994). The schizont stage of *T. parva* resides within leukocytes and has direct contact with the host-cell cytoplasm and matrix. *T. parva* is among several parasites that inhibit host-cell apoptosis pathways to ensure their intracellular survival (Heussler et al., 2001b). The parasites have the unique ability to transform host lymphocytes and to synchronize their division with that of the host cell (Hulliger et al., 1964; von Schubert et al., 2010), ensuring that infection is maintained in daughter lymphocytes. Parasite multiplication is dependent on host-cell proliferation. The transformation and immortalization of *T. parva*-infected cells is very reminiscent of tumor cells, a major difference being that *T. parva*-induced transformation is reversible, as leukocytes return to a resting phenotype upon elimination of the parasite by the anti-parasitic agent buparvaquone. This suggests that transformation is not dependent on defined genomic changes in the host cell (Dobbelaere and Heussler, 1999). However, the underlying mechanisms by which *T. parva*-induces incomplete transformation have not been defined.

p53 acts as a tumor suppressor in mammalian cells reviewed in (Gottlieb and Oren, 1996). Under normal conditions, p53 is maintained at low levels due to its rapid turnover and degradation by proteasomes (Vogelstein et al., 2000). In response to diverse types of stress, p53 can accumulate and can influence cell cycle progression. The mouse double minute 2 (*mdm2*) gene was originally identified as an amplified gene on the double-minute chromosome in a spontaneously transformed mouse BALB/c 3T3 cell line (Cahilly-Snyder et al.,

1987). The MDM2 protein acts as a negative regulator of p53 through two known mechanisms: First, MDM2 binds p53 through its NH₂-terminus, resulting in inhibition of its transcriptional activity (Momand et al., 1992), and second, the COOH-terminus of MDM2 serves as an E3 ubiquitin ligase targeting p53 for proteasomal degradation (Haupt et al., 1997). MDM2 can exhibit oncogenic activity when overexpressed in cells (Fakharzadeh et al., 1991), and gene amplification and overexpression of MDM2 protein are found in about 10% of human tumors (Toledo and Wahl, 2006). In addition, many spliced isoforms of MDM2 are observed in human tumors, and the cDNA coding some of these spliced isoforms is also capable of transforming cells (Sigalas et al., 1996). Thus, both overexpression and alternative splicing of MDM2 are thought to contribute to its oncogenic function.

In this study, we screened *T. parva*-infected lymphocytes for susceptibility to a library of compounds with known anti mitotic activity in an attempt to identify signaling pathways involved in causing parasite-induced unlimited cell proliferation.

TIBC is an anticancer agent that has been suggested to affect the MDM2/p53 protein complex to selectively inhibit the growth of MDM2-overexpressing tumors (Kumar et al., 2003). The anti-tumor effects of TIBC, which have been confirmed in cancers *in vitro* and *in vivo* (Sasayama et al., 2007), has shown some promise for chemotherapeutic use, especially against tumors in which MDM2 overexpression occurs in the absence of genomic mutations in p53. In this study, we found that the TIBC specifically and efficiently inhibited proliferation of *T. parva*-infected lymphocytes, leading to apoptosis. We analyzed the MDM2 and p53 status of several *T. parva*-infected cell lines with respect to mRNA and/or protein expression levels to elucidate the fundamental mechanisms of incomplete transformation of lymphocyte induced by intracellular infection of *T. parva*.

Materials and methods

Cell culture

Cell lines infected with the Muguga or Marikebuni stocks of *T. parva* (Brown and Logan, 1986) were derived by *in vitro* infection of peripheral blood mononuclear cells (PBMC) or in one case (G6TpM, provided by Dr. R. Bishop, International Livestock Research Institute, Nairobi, Kenya) a cloned bovine T lymphoblastoid cell line, with sporozoites. Two of the lines (951-I38TPMa and 951-E43TPMa), derived from the same animal, had been cloned by limiting dilution and contained genotypically distinct parasite clones (Katzner et al., 2006). The designated numbers (592, 011, 641, or 951) indicate animal numbers of healthy Holstein cattle from which blood was collected. Control uninfected activated lymphocytes were prepared by stimulation of PBMCs from the same animals (011, 641, and 951) with concanavalin A (ConA; 0.5 µg/ml). *T. parva*-infected cell lines were maintained in RPMI-1640 culture medium containing 10% heat-inactivated fetal bovine serum

(FBS), 50 μ M 2-mercaptoethanol, 50 units/ml penicillin, and 50 μ g/ml streptomycin. For maintenance of ConA-treated lines, 10 U/ml recombinant mouse IL-2 (R&D Systems) was also added to the medium. Madin Darbey bovine kidney (MDBK) cells and a bovine leukemia transformed cell line BTL-26 (kindly provided by Dr. N. Ishiguro, Gifu University, Japan) (Komori et al., 1996) were grown in Dulbecco's modified Eagle's medium supplemented with 10% FBS, 50 units/ml penicillin, and 50 μ g/ml streptomycin. To eliminate *T. parva* schizonts from the infected cells (011TPM), cells were cultured with 100 ng/ml buparvaquone (Butalex; Essex Animal Health) in the presence of 100 U/ml recombinant mouse IL-2 for 2 or 5 days. Studies involving the use of animals were conducted under a Project Licence issued by the UK Home Office and all experimental procedures were approved by the University of Edinburgh Animal Ethics Committee. The number of the Home Office Licence under which the work was carried out is 60/3736.

Screening of compounds for inhibition of *T. parva*-infected cell proliferation

Cell proliferation assays were performed to examine whether anticancer compounds affected growth of *T. parva*-infected lymphocytes. The SCADS inhibitor kits I and II, consisting of 190 kinds of inhibitors, were kindly provided by the Screening Committee of Anticancer Drugs supported by Grant-in-Aid for Scientific Research on Priority Area "Cancer" from The Ministry of Education, Culture, Sports, Science and Technology, Japan. These compounds were added to 5×10^4 *T. parva*-infected G6TpM cells or ConA-stimulated lymphocytes in 96-well plates at a concentration of 10 μ M, then proliferation was quantified after 24 h incubation using a BrdU proliferation ELISA kit (Roche) according to the manufacturer's instructions.

Effects of TIBC on cell death and p53 expression in *T. parva*-infected lymphocytes

G6TpM cells (1.5×10^5), BTL-26 cells and MDBK cells were treated with TIBC (Merck-Calbiochem) for 50 h in 24-well plates. For the detection of apoptotic cells, cells were stained with propidium iodide (PI) and Allophycocyanin-conjugated annexin V (BD Biosciences), and analyzed by flow cytometry on a FACSCanto cell analyzer (BD Biosciences). 011TPM, 951-E43TPMa, and 951ConA cells were similarly treated with TIBC in 24-well plates, and 2×10^4 cells from each treatment group were then transferred to a 96-well white plate. To indicate apoptosis, the activity of caspase 3 and 7 was quantified using the Caspase-Glo 3/7 kit (Promega) according to the manufacturer's instructions. Luminescence was measured with a luminometer (Victor; PerkinElmer). For the induction of DNA damage, 5×10^5 G6TpM, BTL-26, and MDBK cells were treated with cisplatin (Merck-Calbiochem) for 24 h at 0, 5, 20 or 50 μ M in 8-well plates, and subjected to Western blot analysis as described below. For detection of p53 protein or the transcript of its downstream target Bax, 5×10^5 G6TpM was treated with TIBC for 50 h at 0, 5, 10 or 25 μ M in 8-well plates. Cells were harvested, and Western blot analysis was performed as described below.

RT-PCR for detection of spliced isoforms of *mdm2*

Total RNA was isolated from cells by the PureLink Micro-to-Midi Total RNA Purification System (Invitrogen). cDNAs were then synthesized from total RNA in the presence of oligo(dT) primers using a Ready-To-Go You-Prime First-Strand Beads kit (GE Healthcare) in accordance with the manufacturer's instructions. The resulting cDNAs were used in nested PCR to detect *mdm2*. Nested PCR primers were designed based on the bovine *mdm2* sequence, mdm2F1 (5'-AACTGGGGAGCCTCGGGGA-3') and mdm2R1 (5'-GGTATTATCTTGCTTTGATACACCT-3') for the first amplification, and mdm2F2 (5'-GTTAGTGAGCATCAGGCAAATGTG-3') and mdm2R2 (5'-TTACAGGTAGTTCAACTAGGGG-3') for the second amplification. Each PCR was performed under the following conditions: 95°C for 1 min, 25 amplification cycles (95°C for 1 min, 55°C for 1 min, and 72°C for 1 min), and a final extension step (72°C for 7 min). As an internal control, GAPDH amplification was performed with BoGAPDH-F (5'-TTCAACGGCACAGTCAAGG-3') and BoGAPDH-R (5'-ACATACTCAGCACCAGCATCAC-3'), using the conditions described above, except for the annealing temperature, which was 57°C. Amplification of the *mdm2b* isoform was also performed using specific primers (BoMBforward: 5'-AAGAGACCCTGGACTATTGGAAGTG-3' and BoMBreverse: 5'-TGCCATTGAACCTTGTGTGATTTG-3') after a first amplification with mdm2F1 and mdm2R1, as previously described (Steinman et al., 2004). For *mdm2b* isoform detection, a 30 amplification cycle was used while the rest of the PCR protocol remained the same as above. The PCR products were resolved on 1.2% agarose gels, isolated, cloned into the pGEM-T Easy Vector system (Promega), and sequenced in an ABI Prism 3700 Analyzer (Applied Biosystems).

Quantitative RT-PCR

The levels of transcription of *mdm2* and p53 were determined by quantitative RT-PCR with SYBR Premix Ex Taq (Takara) and Eva Green dye (Biotium). Values were normalized to the value of GAPDH. Primer sequences were as follows; MDM2: 5'-GGCATGCTTCACATGTGCAA-3' and 5'-GTACAATCATTGAATTGGTTGCC-3'; p53: 5'-ACTGGAAGACTCTTGTGGTAACCT-3' and 5'-TTTTCTTCCTCAGTGCGGCGGTC-3'; GAPDH: 5'-GGTCATCATCTCTGCACCTTCTG-3' and 5'-AGGGTGTGTTATACTTCTCGTGG-3'. Standard curves were constructed for all amplicons and each measurement was performed in triplicate. The reaction was performed at 95°C for 10 s, followed by 40 amplification cycles (95°C for 10 s, 60°C for 20 s) in a Mx3000P Real-Time PCR System (Stratagene).

Western blot analysis

Whole cell extracts were lysed in a lysis buffer (0.5% TritonX-100, 50 mM Tris-HCl [pH7.4], 150 mM NaCl) supplemented with a protease inhibitor cocktail (Complete Mini; Boehringer Mannheim) at 4°C for 10 min, and centrifuged. Supernatants were resuspended in a sample buffer for sodium dodecyl sulfate polyacrylamide gel electrophoresis (SDS-PAGE) and heated at 100°C for 3 min. The concentrations of the proteins were estimated using the BCA Protein Assay Reagent (Thermo Scientific) or Quant-iT Protein Assay kit (Invitrogen). Proteins from each sample (30 µg) were subjected to electrophoresis in a polyacrylamide gel, and separated proteins were transferred to a sheet of PVDF membrane (Bio-Rad Laboratories). The filters were blocked in 5% skim milk powder in Tris-buffered saline with 0.1% Tween 20 (TBS-T) for 1 h at room temperature, and washed with TBS-T three times for 10 min each. The filters were incubated with primary antibodies overnight at 4°C, washed, and incubated for 1 h at room temperature with horseradish peroxidase-conjugated goat anti-mouse antibody (Zymed laboratories, cat. no. 62-6420; 1:3,000) or goat anti-rabbit antibody (Jackson ImmunoResearch, cat. no. 111-036-045; 1:6,000). The bands were visualized with SuperSignal West Femto Maximum sensitivity substrate (Thermo Scientific). Membranes were reprobed with another antibody after they were stripped with Restore Western Blot Stripping Buffer (Thermo Scientific). Antibodies used in this study were anti-MDM2 (N20; 1:1,000; Santa Cruz), anti-p53 (PAb421; 1:1,000; Merck-Calbiochem), anti-Bax (Poly6251; 1:3,000; BioLegend), and anti-β-actin (C4;1:3,000; Santa Cruz Biotechnology).

Immunostaining

For staining of MDM2, cytospin smears of *T. parva*-infected cells (G6TpM) were fixed with 4% paraformaldehyde/PBS at room temperature for 15 min, permeabilized with 0.2% Triton X-100 for 10 min and blocked with 5% skimmed milk for 1 h, before staining with anti-MDM2 (N20 diluted 1:500) for 1 h at room temperature followed by Alexa 594-conjugated anti-rabbit Ig (Invitrogen). Immunostaining for p53 was performed essentially as described by Haller *et. al.* (Haller et al., 2010). The slides were fixed with 3% paraformaldehyde/PBS for 10 min, permeabilized with 0.25% Triton X-100 for 10 min, blocked with 10% bovine serum albumin in PBS for 30 min, stained with anti-p53 (OP33, Calbiochem; 1:2000) overnight at 4°C, and detected with Alexa 555-conjugated anti-mouse Ig (Invitrogen). DAPI (blue) was used for nuclear staining.

Reporter assay

To determine p53 activity in the cells, 5×10^5 *T. parva*-infected cells (G6TpM) and BTL-26 cells in 24-well plates were co-transfected with 500 ng of a p21 luciferase reporter plasmid (Shimizu et al., 2002) and a control plasmid containing Renilla luciferase pGL4.70 (25 ng; Promega). After 12 h, cisplatin or TIBC was added to the culture, and cells were incubated for an additional 24 h. Transfection was performed with the Neon

Transfection System (Invitrogen) at 1300 V, 30 ms pulse width and one-time pulse. These conditions were optimized to achieve high levels of efficiency and viability (data not shown). Both firefly and Renilla luciferase activity was assayed with the Dual-Luciferase Reporter Assay System (Promega) and measured with a GloMax luminometer (Promega). The firefly signal was normalized using the Renilla luminescence signal.

Results

Identification of signaling pathway related to proliferation of *T. parva*-infected lymphocytes

We examined the effects of various chemical inhibitors using the SCADS inhibitor kits I and II, which consist of 190 inhibitors. In the first screening, 65 compounds were found to inhibit proliferation of *T. parva* (G6TpM)-infected cells by >90% compared with cells mock-treated with DMSO. To exclude compounds with nonspecific cytotoxic activity, we carried out a second screening of these 65 compounds comparing their effect on *T. parva* (G6TpM)-infected and ConA-stimulated lymphocytes. Thirty-six compounds, targeting different signaling pathways, have shown to have specific effects on proliferation of *T. parva*-infected lymphocytes when compared with ConA-stimulated lymphocytes as listed in Table 1.

The MDM2 inhibitor TIBC specifically induce apoptosis in *T. parva*-infected lymphocytes

MDM2 is well-recognized oncoprotein that participates in the induction of malignant lymphoma when overexpressed in mice (Jones et al., 1998). MDM2 has not previously been studied in *T. parva* infection. The ability of the MDM2 inhibitor TIBC to induce apoptosis of *T. parva*-infected lymphocytes was examined. The *T. parva*-infected and non-infected cell lines used in this study are summarized in Table 2. *T. parva*-infected G6TpM cells displayed susceptibility to TIBC at high concentrations, exhibiting high levels of apoptosis, whereas the bovine leukemia cell line BTL-26 and MDBK cell line remained unaffected (Fig. 1A). The effects of TIBC on other *T. parva*-infected cells, including a different stock of *T. parva* (Marikebuni stock) and uninfected bovine lymphocytic cells (listed in Table 2) were further investigated. As shown in Fig. 1B, *T. parva*-infected cell lines (011TPM and 951-E43TPMa) were highly susceptible for TIBC induced apoptosis. Discernible pathologic effects were not observed in non-infected cells (951ConA) at the concentration used in the experiment. These results suggest that MDM2 participates in maintaining the immortalization of *T. parva*-infected lymphocytes.

Isolation of spliced *mdm2* isoforms from *T. parva*-infected lymphocytes

The complete coding region of bovine *mdm2* was isolated from a cDNA obtained from *T. parva*-infected G6TpM cells by nested RT-PCR (Fig. 2A). The bovine MDM2 amino acid sequence predicted

from the resultant cDNA sequence showed 94% amino acid identity with human MDM2 (HDM2; GenBank accession number NM_002392; Fig. 3A). Analysis of the *mdm2* PCR products from *T. parva*-infected lymphocytes revealed several shorter products in addition to an increased amount of the product corresponding to the full-length transcript (Full-*mdm2*), whereas no such changes to the amplification were observed in ConA cell lines 641 and 951, BTL-26 and MDBK cells (Fig. 2A). Cloning and sequencing of these RT-PCR products from *T. parva*-infected G6TpM cells led to identification of 4 alternatively spliced isoforms of *mdm2* transcripts from *T. parva*-infected lymphocytes, which were designated *mdm2-TPalpha* (GU951438), *mdm2-TPFL7* (GU323559), *mdm2-R3U* (GU323560), and *mdm2-TPR3L* (GU323561). Two of these corresponded to transcripts described previously in other species (Fig. 3A): *Mdm2-TPalpha* contained an insert of 87 bp between exon 4 and 5, and this additional sequence contained a stop codon in-frame. This transcript corresponds to *mdm2α* identified from PBMC in human and dog (Veldhoen et al., 1999) and to *mdm2-DS3* obtained from a soft tissue sarcoma (Bartel et al., 2001). This alpha domain sequence and the insertion sites found to be highly conserved between the human, canine, and bovine products (Fig. 3A). The *mdm2-TPalpha* sequence is predicted to disrupt the p53 binding domain of the MDM2 protein. The second splice variant, *mdm2-TPFL7*, in which exon 5 was aberrantly spliced to exon 12, corresponds to *mdm2-FB28* identified in pediatric rhabdomyosarcoma (Bartel et al., 2001). In the two novel alternatively spliced transcripts of MDM2, *mdm2-TPR3U* and *mdm2-TPR3L*, exon 4 was aberrantly spliced to exon 12. *Mdm2-TPFL7* and *mdm2-TPR3L* caused a frame shift in the region encoding the C-terminus, resulting in completely new predicted amino acid sequences and loss of the RING domains, whereas *mdm2-TPR3U* and *mdm2-TPalpha* retain these domains. Because *mdm2b* (HSU33200) is the most commonly found spliced isoform of *mdm2* in numerous types of cancer cells (Bartel et al., 2002), and it can induce cell transformation independently of p53 (Steinman et al., 2004), we examined transcription of bovine *mdm2b* by nested RT-PCR using *mdm2b*-specific primers, as described previously (Steinman et al., 2004). The *mdm2b* transcript is aberrantly spliced from exon 3 to exon 12. *mdm2b* transcripts were detected in *T. parva*-infected cell lines tested, but only a faint band were detected in uninfected ConA-stimulated lymphocytes (Fig. 2B), suggesting that an elevation of *mdm2b* mRNA levels is associated with *T. parva* infection.

MDM2 is overexpressed in cells infected with *T. parva*

MDM2 is overexpressed in various tumors, and TIBC and nutlin-3 are effective at inhibiting the growth of MDM2-overexpressing cells, such as breast cancer cells (Kumar et al., 2003), glioma cells (Sasayama et al., 2007), and human pediatric acute lymphoblastic leukemia cells (Gu et al., 2008). The finding that *T. parva*-infected lymphocytes are sensitive to MDM2 inhibitors led us to investigate protein expression levels of MDM2. We performed Western blot analysis with anti-MDM2 antibody (N20) and found that *T. parva*-infected

cells had increased MDM2 levels, compared to ConA-stimulated lymphocytes (Fig. 4A). As observed for sensitivity to TIBC, the expression levels of MDM2 varied depending on the parasitized cell line examined. The highest expression level of MDM2 was observed in the 592TPM cell line (*T. parva* -infected B cell line). Since *Theileria* infection does not always result in the same patterns of host cell signaling pathway activation in cell lines of different phenotype (Guergnon et al., 2003; Rocchi et al., 2006), this variation in expression levels of MDM2 may be due to difference in host cell phenotype and/or the parasite species or strain. Elimination of the parasite by treatment with the theilericidal drug buparvaquone led to the disappearance of the MDM2 bands (Fig. 4B). No obviously elevated levels of MDM2 expressions were observed in BTL-26 or MDBK cells (Fig. 4C). Because the *T. parva*-infected cell lines express several alternative transcription variants, next we evaluated transcript abundance of *mdm2* mRNA including transcription isoforms by quantitative RT-PCR, and the expression levels were normalized against glyceraldehyde-3-phosphate dehydrogenase (*GAPDH*). The primer pair for *mdm2* quantitative RT-PCR is able to detect not only full-length *mdm2* but also other three p53 binding domain defective transcription variants, *mdm2-TP α* , *mdm2-TPR3U* and *mdm2-TPb*. The transcription levels of all *T. parva*-infected cells were more than three times higher than those of any ConA blast or BTL-26 cells (Fig. 4D and E). Various forms of MDM2 are over expressed in *T. parva*-infected cells.

p53 accumulation in response to DNA damage is disordered in *T. parva*-infected lymphocytes

Cisplatin binds to DNA and forms platinum-DNA adducts, resulting in p53 accumulation and induction of apoptosis (Siddik, 2003). To examine p53 protein activity in *T. parva*-infected lymphocytes, expression in *T. parva*-infected and uninfected cell lines prior to and/or after (24h) treatment with cisplatin was compared by Western blot analysis. In both uninfected cell lines (BTL-26, MDBK cells), the levels of p53 increased after treatment with cisplatin, whereas the *T. parva*-infected cells (G6TpM) showed no apparent accumulation of p53 protein following cisplatin-treatment (Fig. 5A). The transcription levels of p53 were also determined by quantitative RT-PCR in *T. parva*-infected cells (G6TpM), BTL-26 cells, and MDBK cells after treatment with cisplatin. Transcription of p53 was further upregulated in the *T. parva*-infected cells by the cisplatin treatment, but was unaffected in the two uninfected cell lines (Fig. 5B). In addition, p21-luciferase reporter assay indicated that p53 activities after cisplatin treatment in *T. parva*-infected cells remained unaffected despite those in control BTL-26 cells increased in dose dependent manner (Fig. 5C), consistent with the results of Western blot analysis in Fig. 5a. These observations indicate that p53 protein accumulation and activity is impaired in *T. parva*-infected lymphocytes.

TIBC restores the p53 response in *T. parva*-infected lymphocytes

To determine whether impairment of p53 accumulation was associated with MDM2 overexpression,

we examined the status of p53 after treatment with TIBC. Western blot analysis showed an increased level of p53 protein after 24 h of exposure to TIBC in *T. parva*-infected cells (G6TpM). Expression of the pro-apoptotic molecule Bax, a p53 target, was also elevated in G6TpM cells (Fig. 5D), indicating that the p53 pathway remained functional in *T. parva*-infected lymphocytes and could be restored by inhibiting MDM2 activity. Consistent with the restoration of p53 protein, increased p53 activity in TIBC-treated *T. parva*-infected G6TpM cells was also confirmed using a p21-reporter plasmid assay as shown in Fig. 5C.

Nuclear accumulation of p53 were induced by TIBC treatment

Activation of p53 is accompanied by its stabilization and nuclear accumulation by MDM2. To determine cellular the distribution of p53 after abrogation of MDM2 function, *T. parva*-infected cells were stained with anti-p53 before and after treatment of TIBC for 48 h. While untreated cells showed undetectable levels of p53 protein, TIBC treatment for 48 h lead to the accumulation of p53 in nucleus, most likely in the nucleoli (Fig. 6A). On the other hand, MDM2 were distributed mainly in the nucleoplasm (Fig. 6B upper). Disappearance of MDM2 staining signals in the cells which showed typical apoptotic morphological changes of nucleus (arrowhead) after induction of apoptosis by theilericidal drug buparvaquone were observed, indicating that the expression of MDM2 is regulated by the presence of the parasite.

Discussion

Transformation features of *T. parva*-infected lymphocytes are sensitive to the MDM2 inhibitor TIBC. Infected cells express high levels of MDM2 and have several alternatively spliced *mdm2* transcripts. The overexpression of MDM2 protein in *T. parva*-infected cells was associated with enhanced transcription or increased stability of *mdm2* mRNA as demonstrated by real-time RT-PCR. MDM2 is an oncoprotein that controls tumorigenesis through both p53-dependent and p53-independent mechanisms (Bartel et al., 2002). It is known that the p53-dependent mechanism involves inhibition of p53 activity by MDM2, by direct-binding (Momand et al., 1992), shuttling p53 from the nucleus to the cytoplasm (Tao and Levine, 1999), and inducing ubiquitination and hence degradation by the ubiquitin-proteasome system (Haupt et al., 1997). Several lines of evidence support a role for p53-independent functions of MDM2 in tumor formation (Bouska et al., 2008; Ganguli and Wasylyk, 2003).

p53 is a major regulator of cell homeostasis in response to insults such as radiation damage, microbial infection, or tumorigenesis (del Aguila et al., 2006; Teodoro and Branton, 1997; Vousden and Lu, 2002). Oncogenes that deliver strong mitogenic signals cause cellular senescence that arrests cell proliferation or causes apoptosis by the p53-dependent pathway (Yaswen and Campisi, 2007). Because *Theileria* infection results in strong mitogenic stimulation and the majority of infected cells retain wild-type p53, activation of p53

might be expected to retard proliferation and allow elimination of the infected cells. However, *T. parva*-infected cells acquire the ability to proliferate indefinitely, avoiding cell-cycle arrest and apoptosis. Indeed, a recent study by Haller *et al.* (2010) demonstrated that p53-mediated host cell apoptosis is suppressed during *Theileria* infection, but is rapidly re-activated after elimination of the parasite by the anti-parasitic drug treatment (Haller *et al.*, 2010). Notably, we detected an mRNA in *T. parva*-infected lymphocytes predicted to encoding a protein homologous to *mdm2b*, which has been reported to have p53-independent tumorigenicity (Steinman *et al.*, 2004). Among 5 spliced isoforms of *mdm2* detected in *T. parva*-infected lymphocytes, three of them corresponded to previously reported spliced isoform sequences of *mdm2* (*mdm2-TP2b* corresponded to human *mdm2b*, *mdm2-TP α* corresponded to human *mdm2 α* , and *mdm2-TPFL7* corresponded to *mdm2-FB28* from human rhabdomyosarcoma), whereas the other two isoforms (*mdm2-TPR3U* and *mdm2-TPR3L*) were novel. The predicted protein products of all of them lacked the p53-binding domain, but *mdm2-TP α* , *mdm2-TPR3U*, and *mdm2-TP2b* still bore the RING finger domain at the C-terminus. The C-terminal RING finger domain of MDM2 contains a cysteine residue that is essential for its function as an E3 ubiquitin conjugating enzyme and for its ability to induce degradation of p53 (Honda and Yasuda, 2000). We did not determine whether these spliced isoforms of *mdm2* were expressed as protein species, but we speculate that one or more of the isoforms play some role of incomplete transformation of *T. parva*-infected cells by p53-independent mechanisms. Alternatively, expression of spliced isoforms of *mdm2* may merely be a secondary phenomenon associated with excess transcription of *mdm2*, because spliced forms of *mdm2* mRNA were usually found together with full-length MDM2 transcripts (Bartel *et al.*, 2002).

Upon DNA damage, p53-MDM2 interactions are affected by phosphorylation of p53 (Bode and Dong, 2004). Indeed, in our study, p53 protein was increased after cisplatin treatment in control cells (BTL-26 or MDBK) without an increase in *p53* mRNA transcription, suggesting that p53 levels in these cells were post-transcriptionally controlled by MDM2 preventing the degradation of p53. In contrast, *T. parva*-infected lymphocytes were not responsive to cisplatin-induced p53 accumulation. We noted that *p53* mRNA was upregulated, suggesting that the absence of p53 accumulation is post-transcriptionally controlled, either by translation failure or excessive degradation, rather than the result of a reduced transcription rate. Since MDM2 was aberrantly overexpressed in *T. parva*-infected cells, active degradation of p53 may be the most likely explanation for the defective p53 response. The enhanced transcription of *p53* may be caused by MDM2, which induces p53 translation as a negative feedback loop (Wu X Fau - Bayle *et al.*, 1993). To test the hypothesis that the p53 dysfunction was caused by aberrant MDM2 expression, we examined the status of p53 after treatment with a MDM2 inhibitor. Indeed, the MDM2 inhibitor TIBC rescued normal p53 accumulation with transcriptional function, and caused apoptosis of the *T. parva*-infected lymphocytes, suggesting that over-expression of MDM2 contributed to the perturbation of the p53 pathway.

In our studies, p53 was mainly localized within the nucleus of the infected cells, and the staining signal for p53 in the nucleus was increased after TIBC treatment (Fig. 6A). Other workers have reported that p53 in *T. parva*-infected cells is associated with the schizont membrane (Haller et al., 2010) but how the parasite sequesters p53 to this location was not determined. The reason for the apparent discrepancy between our p53 staining pattern and that obtained by Haller *et al.* is unclear. Haller *et al.* proposed sequestration to the parasite surface as a mechanism for p53-suppression in *Theileria*-infected cells. However, it is uncertain whether all synthesized p53 molecules could be recruited to the parasite surface. It is possible that only p53 protein that evades the p53-degradation process is trapped to the parasite membrane. Considering the consistent expression of intact forms of p53, degradation of p53 by MDM2, in addition to cytoplasmic sequestration, may be required for host cell survival and continued proliferation of the parasite. The findings, from these two studies indicate that *Theileria* might negatively regulate p53 by two means, one by sequestration and another by active degradation of it.

In *T. parva*-infected cells, MDM2 was primarily localized to the host nucleoplasm (Fig. 6B). In untransformed cells, p14^{ARF}-/p19^{ARF} negatively regulates MDM2 by sequestering MDM2 from the nucleoplasm to nucleoli, which results in the accumulation of p53 in the nucleoplasm (Weber et al., 1999). The observed nucleoplasmic localization of MDM2 in the *T. parva*-infected cells might be linked indirectly to altered ARF function by the infection.

. The molecules known to regulate the transcription of *mdm2* include p53 (Juven et al., 1993), AP-1, Ets (Phelps et al., 2003), and PTEN (Chang et al., 2004). The nuclear factor-kappa B (NF-κB) is also a transcription regulator of MDM2 through its binding to the P1 promoter, and has been shown to induce MDM2 expression in mouse embryonic fibroblasts (Tergaonkar et al., 2002) and activated T cells (Busuttill et al., 2010).

Inhibition of the multi-subunit I kappa B kinase suppresses MDM2 expression levels in Epstein Barr virus-infected cells, suggesting that the steady-state protein level of MDM2 can be controlled by NF-κB activity (Forte and Luftig, 2009). NF-κB is constitutively activated in *T. parva*-infected lymphocytes as a consequence of modulation of multi-subunit IκB kinase signalosome complex (Heussler et al., 1999; Heussler et al., 2002; Ivanov et al., 1989). Hence, NF-κB activation may be a key step for constitutive upregulation of MDM2 in *T. parva*-infected lymphocytes.

In addition to NF-κB activation, the phosphoinositide 3-kinase (PI3-K)/Akt pathway may be relevant to functional activation of MDM2. Phosphorylation of MDM2 by Akt/PKB has been reported to result in nuclear translocation of MDM2 (Mayo and Donner, 2001), enhancement of MDM2-mediated ubiquitination of p53 (Ogawara et al., 2002), and stabilization of MDM2 by preventing self-ubiquitination (Feng et al., 2004). Intriguingly, the PI3-K/Akt pathway is also known to be constitutively activated in *T. parva*-infected cells (Heussler et al., 2001a). Thus, constitutive activation of both the NF-κB and the PI3-K/Akt pathway could favor

survival of parasitized cells by promoting MDM2 expression and enhancing its function, as well as stimulating the expression of anti-apoptotic and pro-proliferative genes (Dobbelaere et al., 2000; Dobbelaere and Kuenzi, 2004; Shiels et al., 2006).

Our results indicate that enhanced expression of MDM2 in *T. parva*-infected cells alters p53 stabilization. These results document a mechanism by which incomplete transformation of cells occurs as a consequence of pathogenic infection by protozoa.

Acknowledgments

We thank Dr. R. Bishop for providing the *T. parva* (Muguga stock)-infected G6TpM cell line. We also thank Dr. N. Ishiguro for providing BTL-26 cell line. This work was supported in part by the Grants-in-Aid for Scientific Research and Asia-Africa S & T Strategic Cooperation Promotion Program by the Special Coordination Funds for Promoting Science & Technology, from the Ministry of Education, Culture, Sports, Science and Technology of Japan (MEXT) to CS. KH was supported by the Program of Founding Research Centers for Emerging and Reemerging Infectious Diseases, MEXT.

Figure Legends

Fig. 1 Apoptotic effects of the MDM2 inhibitor TIBC on *T. parva*-infected lymphocytes. (A) *T. parva*-infected lymphocytes (G6TpM), BTL-26 cells, and MDBK cells were treated with TIBC for 50 h at the indicated concentrations. After 50 h, the percentage of apoptotic cells was determined by flow cytometry after annexin V staining. Annexin V-positive cells were considered to be apoptotic (including cells in early apoptosis and late apoptosis/necrosis). Experiments were repeated three times, and the mean results of three experiments are shown. Error bars represent SD (n = 3). (B) 011TPM, 951-E43TMA, and 951ConA cells were treated with TIBC for 48 h. After 48 h treatment, the degree of apoptosis was determined by measuring the activity of caspase 3 and 7, which is shown as the fold increase over cells mock-treated with DMSO. A representative result of three independent experiments is shown.

Fig. 2 Identification of alternatively spliced isoforms of *mdm2* in *T. parva*-infected lymphocytes. (A) Semiquantitative RT-PCR analysis of *mdm2* expression in *T. parva*-infected lymphocytes or uninfected cells. Expression of mRNA for *mdm2* and *gapdh* was evaluated by RT-PCR. The position of the full-length *mdm2* transcript (1513 bp) is indicated by an arrow. Several shorter products considered to be spliced isoforms of *mdm2* are shown with a bracket. (B) *Mdm2b* was detected in *T. parva*-infected lymphocytes by a set of primers specific for bovine *mdm2b*. Expression of *mdm2b* mRNA, which is one of the spliced isoforms of *mdm2*, was evaluated by nested RT-PCR using *mdm2b*-specific primers. GAPDH amplification was performed as an internal

control.

Fig. 3 Comparison of the nucleotide sequences of spliced *mdm2* isoforms. (A) Alignment of MDM2 amino acid sequences identified in *T. parva*-infected lymphocytes and related genes. GenBank accession numbers or references for the genes are MDM2-TPalpha (GU951438), MDM2-TPR3U (GU323560), MDM2-TPR3L (GU323561), MDM2-TPFL7 (GU323559), FB28 (AF385324), human MDM2b (NM_006879), and canine alpha domain. The arrow indicates positions of bovine *mdm2b*-specific forward primer. (B) Schematic representation of the full-length transcript and spliced isoforms of *mdm2* isolated from *T. parva*-infected lymphocytes. The arrow shows the transcription start site, and the indicated exon numbers correspond to those in human/mouse *mdm2*. Dotted lines indicate splicing connections.

Fig. 4 MDM2 is overexpressed in *T. parva*-infected lymphocytes. (A) Western blot analysis of MDM2 using an antibody specific for MDM2 (N20 from Santa Cruz). The N20 antibody was raised against an N-terminal fragment of human MDM2 and can recognize most spliced isoforms of MDM2 because the N-terminus is retained in the splice variants. NS = nonspecific. Arrows indicate 90-kDa forms of MDM2. (B) Expression of MDM2 after parasite elimination. To eliminate the parasite from the cell, the theilericidal drug buparvaquone (100 ng/ml) was added to TPM011 cells for 2 or 5 days in the presence of 10 U/ml IL-2. Cell lysates were subjected to Western blot analysis for MDM2 and β -actin as a loading control. (C) Expression of MDM2 in *T. parva*-infected or non-infected cells. G6TpM, BTL-26, and MDBK cells were analyzed by Western blot analysis for their expression levels of MDM2 and beta-actin as a loading control. (D) Transcripts of *mdm2* from *T. parva*-infected or ConA-stimulated lymphocytes were quantified using real-time RT-PCR and normalized to GAPDH. Transcription levels of *mdm2* in these cells are expressed as ratios to the level obtained following stimulation of PBMCs from animal 011 with ConA (ConA-011), which was set to 1.0. Experiments were repeated three times, and a representative experiment in triplicate is shown. Bars represent the mean \pm SE (n = 3). (E) Real-time PCR for *mdm2* transcripts in G6TpM, BTL-26, and MDBK cells. The obtained values for *mdm2* were normalized to GAPDH and are shown as ratios of the value obtained in BTL-26 cells. The mean result of the triplicate is shown. Experiments were repeated three times, and representative experiment is shown. Bars represent the mean \pm SE (n = 3).

Fig. 5 Impairment of p53 accumulation after DNA damage in *T. parva*-infected lymphocytes. (A) The status of p53 expression following treatment of cells with cisplatin. *T. parva*-infected lymphocytes (G6TpM), BTL-26 cells, and MDBK cells were treated with cisplatin for 24 h and harvested. Cell lysates were subjected to Western blot analysis using monoclonal antibodies specific for p53 and β -actin (as a loading control). (B) Quantification

of p53 mRNA expression in *T. parva*-infected G6TpM cells following cisplatin treatment. p53 mRNA was quantified by real-time RT-PCR and normalized against GAPDH. The level of transcription obtained with ConA-011 was set to 1, and expression levels in other samples are expressed as ratios relative to that in ConA-011 cells. Bars represent the mean \pm SE (n = 3). (C) Reporter plasmid p21-luciferase together with the control reporter plasmid pGL4.70 was co-transfected into *T. parva*-infected cells (G6TpM) and BTL-26 cells. Cells were incubated with cisplatin or TIBC for 24 h at the indicated concentration 12 h after transfection. Firefly luciferase driven by the p21 promoter was normalized to the control Renilla luciferase activity. The p53 activity in non-treated cells was set to 1, and activity in other cells is expressed as a ratio of this value. Data are representative of three independent experiments. (D) p53 accumulation in *T. parva*-infected cells caused by MDM2 inhibitor TIBC treatment, and subsequent Bax expression. *T. parva*-infected lymphocytes (G6TpM) were treated with the MDM2 inhibitor TIBC for 24 h at the indicated concentrations and harvested. Western blot analysis was performed on cell lysates using antibodies specific for p53, Bax, and β -actin (as a loading control).

Fig.6 Localization of MDM2 and p53 in *T. parva*-infected cells.

(A) *T. parva*-infected cells (G6TpM) were stained with anti-p53 (Red). The weak signals were observed in host nucleus but not in parasite surface (Upper; TIBC 0h). After TIBC treatment for 48 h (Lower; TIBC 48h), the p53 signals (Red) were more detectable at the host nucleus than non-treated cells. (B) *T. parva*-infected cells (G6TpM) were stained with anti-MDM2 (Red). MDM2 was mainly localized to the host nucleoplasm. Host and parasite DNA were stained with DAPI (blue). In the right panel, the merged images of phase-contrast (PC; gray) and the fluorescence signals were shown.

Table 1 List of compounds that affect the proliferation of *T. parva*-infected lymphocytes.

T. parva-infected G6TpM cells and ConA-stimulated bovine lymphocytes were cultured with 10 μ M each of 190 inhibitors (SCADS inhibitor kits I and II) for 24 h, and cell proliferation rates were determined by BrdU-incorporation assay. The list shows 36 compounds that inhibited the proliferation of *T. parva*-infected lymphocytes by >90% compared with cells mock-treated with DMSO, and had specific inhibitory effects on *T. parva*-infected lymphocytes of <30% compared with ConA-stimulated lymphocytes, shown as TP/ConA (%) in this table.

Table2 A list of the cell lines used in this study.

Five *Theileria*-infected cell lines, including cells infected with *T. parva* Muguga and *T. parva* Marikebuni, and five non-infected cell lines were used in this study. Expression of surface markers was analyzed by flow cytometry following staining with bovine monoclonal antibodies directed against CD4 (ILA-12), CD8

(ILA-105), CD3 (MM1A), $\gamma\delta$ (GB21A), and IgM (IL-A30).

References

- Bartel, F., et al., 2002. Alternative and aberrant splicing of MDM2 mRNA in human cancer. *Cancer Cell*. 2, 9-15.
- Bartel, F., et al., 2001. Novel *mdm2* splice variants identified in pediatric rhabdomyosarcoma tumors and cell lines. *Oncol Res*. 12, 451-7.
- Bode, A. M., Dong, Z., 2004. Post-translational modification of p53 in tumorigenesis. *Nat Rev Cancer*. 4, 793-805.
- Bouska, A., et al., 2008. Mdm2 promotes genetic instability and transformation independent of p53. *Mol Cell Biol*. 28, 4862-74.
- Brown, C. G., et al., 1973. Letter: Infection and transformation of bovine lymphoid cells in vitro by infective particles of *Theileria parva*. *Nature*. 245, 101-3.
- Brown, W. C., Logan, K. S., 1986. Bovine T-cell clones infected with *Theileria parva* produce a factor with IL 2-like activity. *Parasite Immunol*. 8, 189-92.
- Busuttill, V., et al., 2010. NF- κ B inhibits T-cell activation-induced, p73-dependent cell death by induction of MDM2. *Proc Natl Acad Sci U S A*.
- Cahilly-Snyder, L., et al., 1987. Molecular analysis and chromosomal mapping of amplified genes isolated from a transformed mouse 3T3 cell line. *Somat Cell Mol Genet*. 13, 235-44.
- Chang, C. J., et al., 2004. PTEN regulates Mdm2 expression through the P1 promoter. *J Biol Chem*. 279, 29841-8.
- del Aguila, C., et al., 2006. Encephalitozoon microsporidia modulates p53-mediated apoptosis in infected cells. *Int J Parasitol*. 36, 869-76.
- Dobbelaere, D., Heussler, V., 1999. Transformation of leukocytes by *Theileria parva* and *T. annulata*. *Annu Rev Microbiol*. 53, 1-42.
- Dobbelaere, D. A., et al., 2000. *Theileria parva*: taking control of host cell proliferation and survival mechanisms. *Cell Microbiol*. 2, 91-9.
- Dobbelaere, D. A., Kuenzi, P., 2004. The strategies of the *Theileria* parasite: a new twist in host-pathogen interactions. *Curr Opin Immunol*. 16, 524-30.
- Fakharzadeh, S. S., et al., 1991. Tumorigenic potential associated with enhanced expression of a gene that is amplified in a mouse tumor cell line. *EMBO J*. 10, 1565-9.
- Feng, J., et al., 2004. Stabilization of Mdm2 via decreased ubiquitination is mediated by protein kinase

- B/Akt-dependent phosphorylation. *J Biol Chem.* 279, 35510-7.
- Forte, E., Luftig, M. A., 2009. MDM2-dependent inhibition of p53 is required for Epstein-Barr virus B cell growth transformation and infected cell survival. *J Virol.* 83, 2491-9.
- Ganguli, G., Wasyluk, B., 2003. p53-independent functions of MDM2. *Mol Cancer Res.* 1, 1027-35.
- Gottlieb, T. M., Oren, M., 1996. p53 in growth control and neoplasia. *Biochim Biophys Acta.* 1287, 77-102.
- Gu, L., et al., 2008. MDM2 antagonist nutlin-3 is a potent inducer of apoptosis in pediatric acute lymphoblastic leukemia cells with wild-type p53 and overexpression of MDM2. *Leukemia.* 22, 730-9.
- Guernon, J., et al., 2003. Apoptosis of *Theileria*-infected lymphocytes induced upon parasite death involves activation of caspases 9 and 3. *Biochimie.* 85, 771-6.
- Haller, D., et al., 2010. Cytoplasmic sequestration of p53 promotes survival in leukocytes transformed by *Theileria*. *Oncogene.* 29, 3079-86
- Haupt, Y., et al., 1997. Mdm2 promotes the rapid degradation of p53. *Nature.* 387, 296-9.
- Heussler, V. T., et al., 2001a. The Akt/PKB pathway is constitutively activated in *Theileria*-transformed leucocytes, but does not directly control constitutive NF-kappaB activation. *Cell Microbiol.* 3, 537-50.
- Heussler, V. T., et al., 2001b. Inhibition of apoptosis by intracellular protozoan parasites. *Int J Parasitol.* 31, 1166-76.
- Heussler, V. T., et al., 1999. The intracellular parasite *Theileria parva* protects infected T cells from apoptosis. *Proc Natl Acad Sci U S A.* 96, 7312-7.
- Heussler, V. T., et al., 2002. Hijacking of host cell IKK signalosomes by the transforming parasite *Theileria*. *Science.* 298, 1033-6.
- Honda, R., Yasuda, H., 2000. Activity of MDM2, a ubiquitin ligase, toward p53 or itself is dependent on the RING finger domain of the ligase. *Oncogene.* 19, 1473-6.
- Hulliger, L., et al., 1964. Mode of Multiplication of *Theileria* in Cultures of Bovine Lymphocytic Cells. *Nature.* 203, 728-30.
- Irvin, A. D., et al., 1975. Comparative growth of bovine lymphosarcoma cells and lymphoid cells infected with *Theileria parva* in athymic (nude) mice. *Nature.* 255, 713-4.
- Ivanov, V., et al., 1989. Infection with the intracellular protozoan parasite *Theileria parva* induces constitutively high levels of NF-kappa B in bovine T lymphocytes. *Mol Cell Biol.* 9, 4677-86.
- Jones, S. N., et al., 1998. Overexpression of Mdm2 in mice reveals a p53-independent role for Mdm2 in tumorigenesis. *Proc Natl Acad Sci U S A.* 95, 15608-12.

- Juven, T., et al., 1993. Wild type p53 can mediate sequence-specific transactivation of an internal promoter within the *mdm2* gene. *Oncogene*. 8, 3411-6.
- Katzer, F., et al., 2006. Extensive genotypic diversity in a recombining population of the apicomplexan parasite *Theileria parva*. *Infect Immun*. 74, 5456-64.
- Komori, H., et al., 1996. Predominant p53 mutations in enzootic bovine leukemic cell lines. *Vet Immunol Immunopathol*. 52, 53-63.
- Kumar, S. K., et al., 2003. Design, synthesis, and evaluation of novel boronic-chalcone derivatives as antitumor agents. *J Med Chem*. 46, 2813-5.
- Lawrence, J. A., Irvin, A. D., Theilerioses. In: J. A. W. Coetzer, et al., Eds.), *Infectious Diseases of Livestock*. Oxford university press, New York, 1994, pp. 307-341.
- Mayo, L. D., Donner, D. B., 2001. A phosphatidylinositol 3-kinase/Akt pathway promotes translocation of Mdm2 from the cytoplasm to the nucleus. *Proc Natl Acad Sci U S A*. 98, 11598-603.
- Momand, J., et al., 1992. The mdm-2 oncogene product forms a complex with the p53 protein and inhibits p53-mediated transactivation. *Cell*. 69, 1237-45.
- Ogawara, Y., et al., 2002. Akt enhances Mdm2-mediated ubiquitination and degradation of p53. *J Biol Chem*. 277, 21843-50.
- Phelps, M., et al., 2003. p53-independent activation of the hdm2-P2 promoter through multiple transcription factor response elements results in elevated hdm2 expression in estrogen receptor alpha-positive breast cancer cells. *Cancer Res*. 63, 2616-23.
- Rocchi, M. S., et al., 2006. The kinetics of *Theileria parva* infection and lymphocyte transformation in vitro. *Int J Parasitol*. 36, 771-8.
- Sasayama, T., et al., 2007. Trans-4-Iodo,4'-boranyl-chalcone induces antitumor activity against malignant glioma cell lines in vitro and in vivo. *J Neurooncol*. 85, 123-32.
- Shiels, B., et al., 2006. Alteration of host cell phenotype by *Theileria annulata* and *Theileria parva*: mining for manipulators in the parasite genomes. *Int J Parasitol*. 36, 9-21.
- Shimizu, H., et al., 2002. The conformationally flexible S9-S10 linker region in the core domain of p53 contains a novel MDM2 binding site whose mutation increases ubiquitination of p53 in vivo. *J Biol Chem*. 277, 28446-58.
- Siddik, Z. H., 2003. Cisplatin: mode of cytotoxic action and molecular basis of resistance. *Oncogene*. 22, 7265-79.
- Steinman, H. A., et al., 2004. An alternative splice form of Mdm2 induces p53-independent cell growth and tumorigenesis. *J Biol Chem*. 279, 4877-86.
- Tao, W., Levine, A. J., 1999. Nucleocytoplasmic shuttling of oncoprotein Hdm2 is required for

- Hdm2-mediated degradation of p53. Proc Natl Acad Sci U S A. 96, 3077-80.
- Teodoro, J. G., Branton, P. E., 1997. Regulation of apoptosis by viral gene products. J Virol. 71, 1739-46.
- Tergaonkar, V., et al., 2002. p53 stabilization is decreased upon NFkappaB activation: a role for NFkappaB in acquisition of resistance to chemotherapy. Cancer Cell. 1, 493-503.
- Toledo, F., Wahl, G. M., 2006. Regulating the p53 pathway: in vitro hypotheses, in vivo veritas. Nat Rev Cancer. 6, 909-23.
- Veldhoen, N., et al., 1999. A novel exon within the mdm2 gene modulates translation initiation in vitro and disrupts the p53-binding domain of mdm2 protein. Oncogene. 18, 7026-33.
- Vogelstein, B., et al., 2000. Surfing the p53 network. Nature. 408, 307-10.
- von Schubert, C., et al., 2010. The transforming parasite *Theileria* co-opts host cell mitotic and central spindles to persist in continuously dividing cells. PLoS Biol. 8. e1000499.
- Vousden, K. H., Lu, X., 2002. Live or let die: the cell's response to p53. Nat Rev Cancer. 2, 594-604.
- Weber, J. D., et al., 1999. Nucleolar Arf sequesters Mdm2 and activates p53. Nat Cell Biol. 1, 20-6.
- Wu X Fau - Bayle, J. H., et al., 1993. The p53-mdm-2 autoregulatory feedback loop. Genes Dev. 7, 1126-32.
- Yaswen, P., Campisi, J., 2007. Oncogene-induced senescence pathways weave an intricate tapestry. Cell. 128, 233-4.

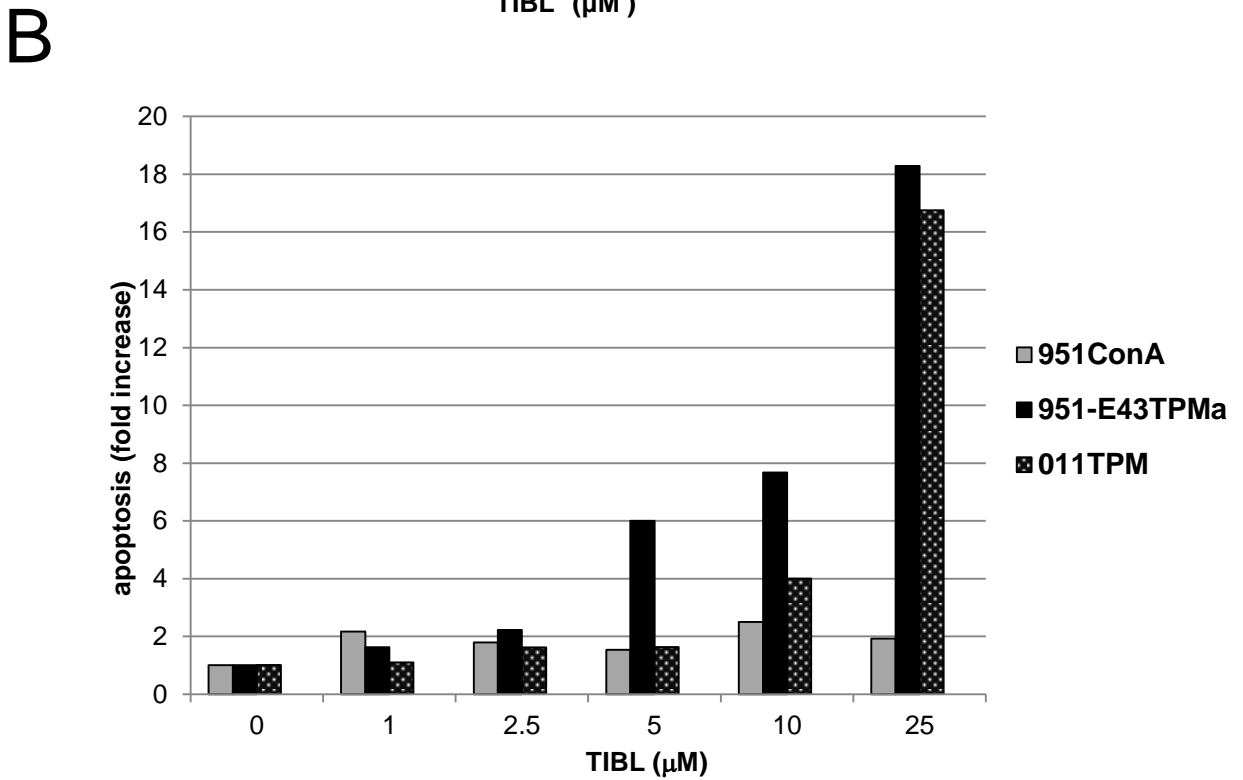
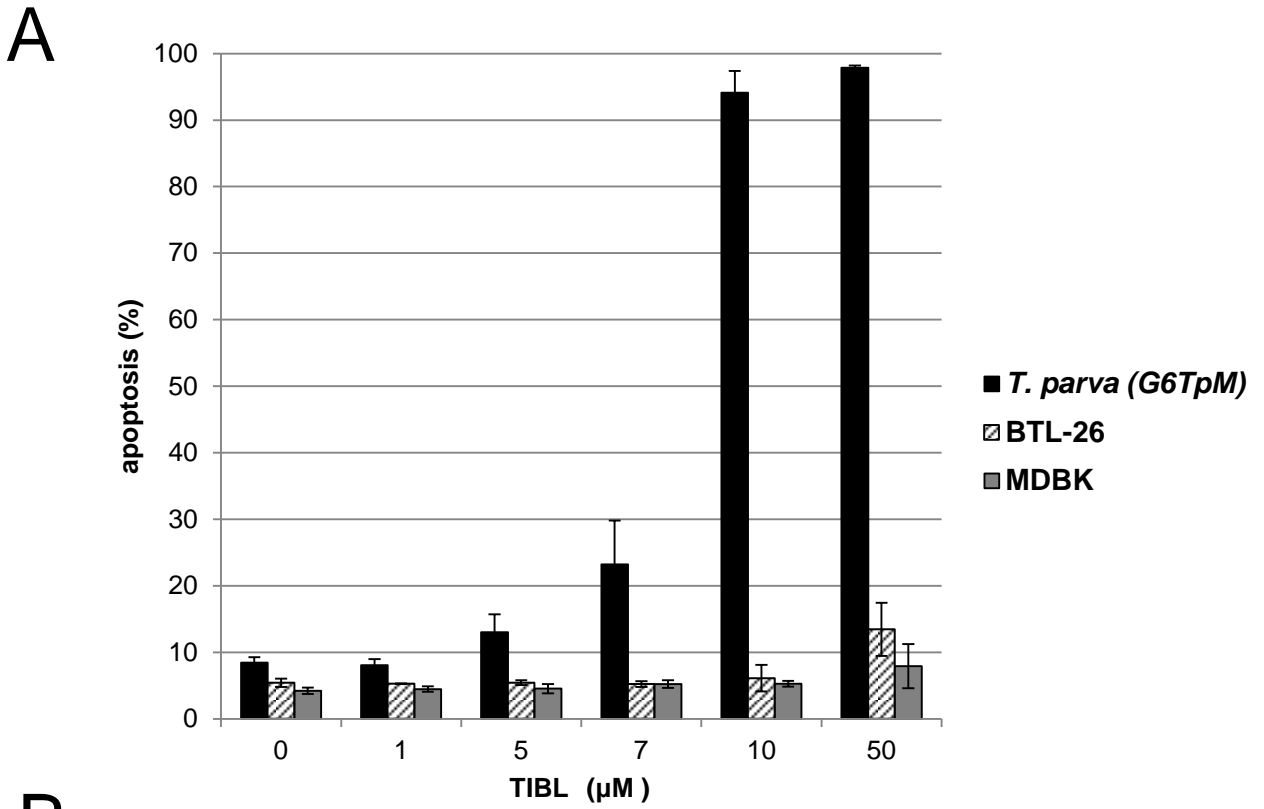
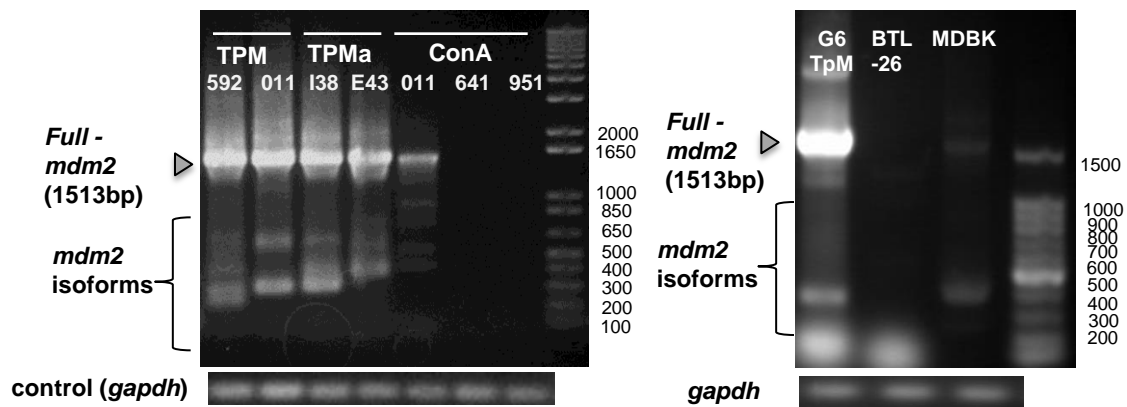


Figure 1

A



B

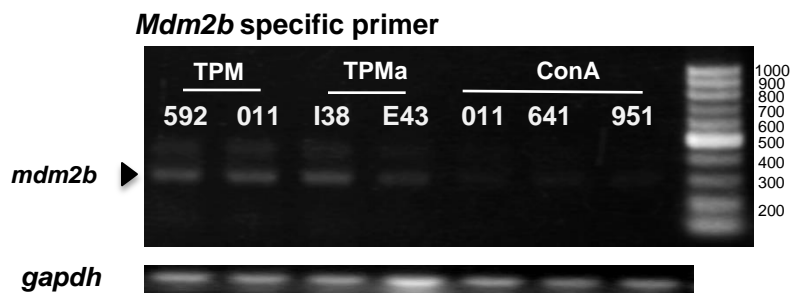
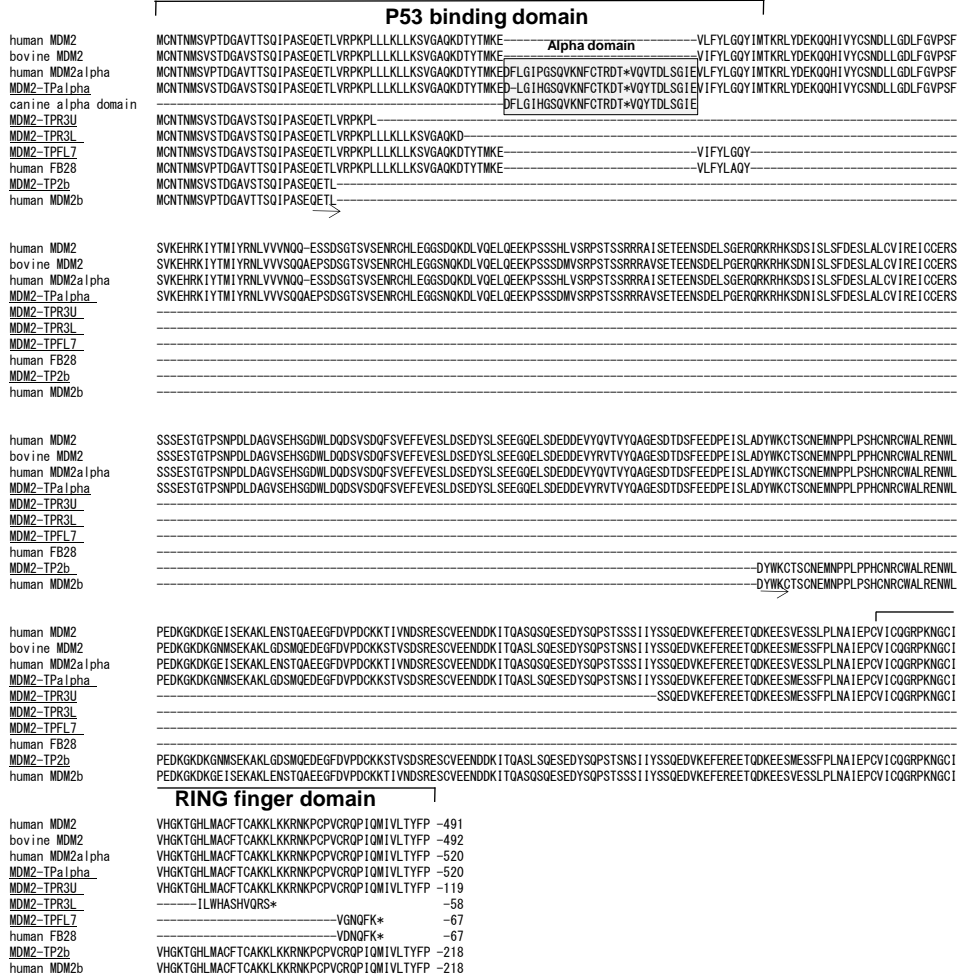


Figure 2

A



B

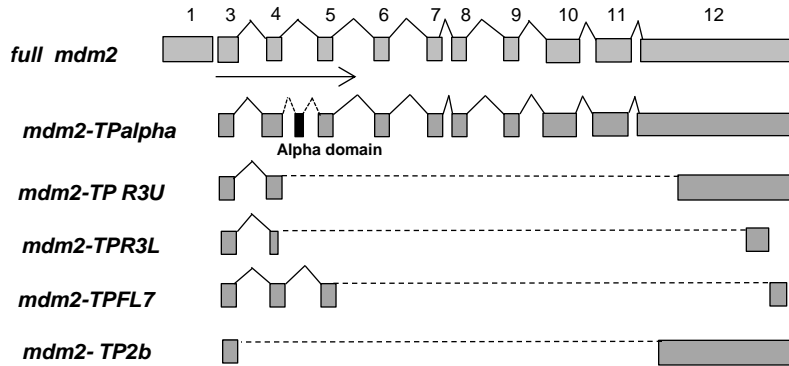


Figure 3

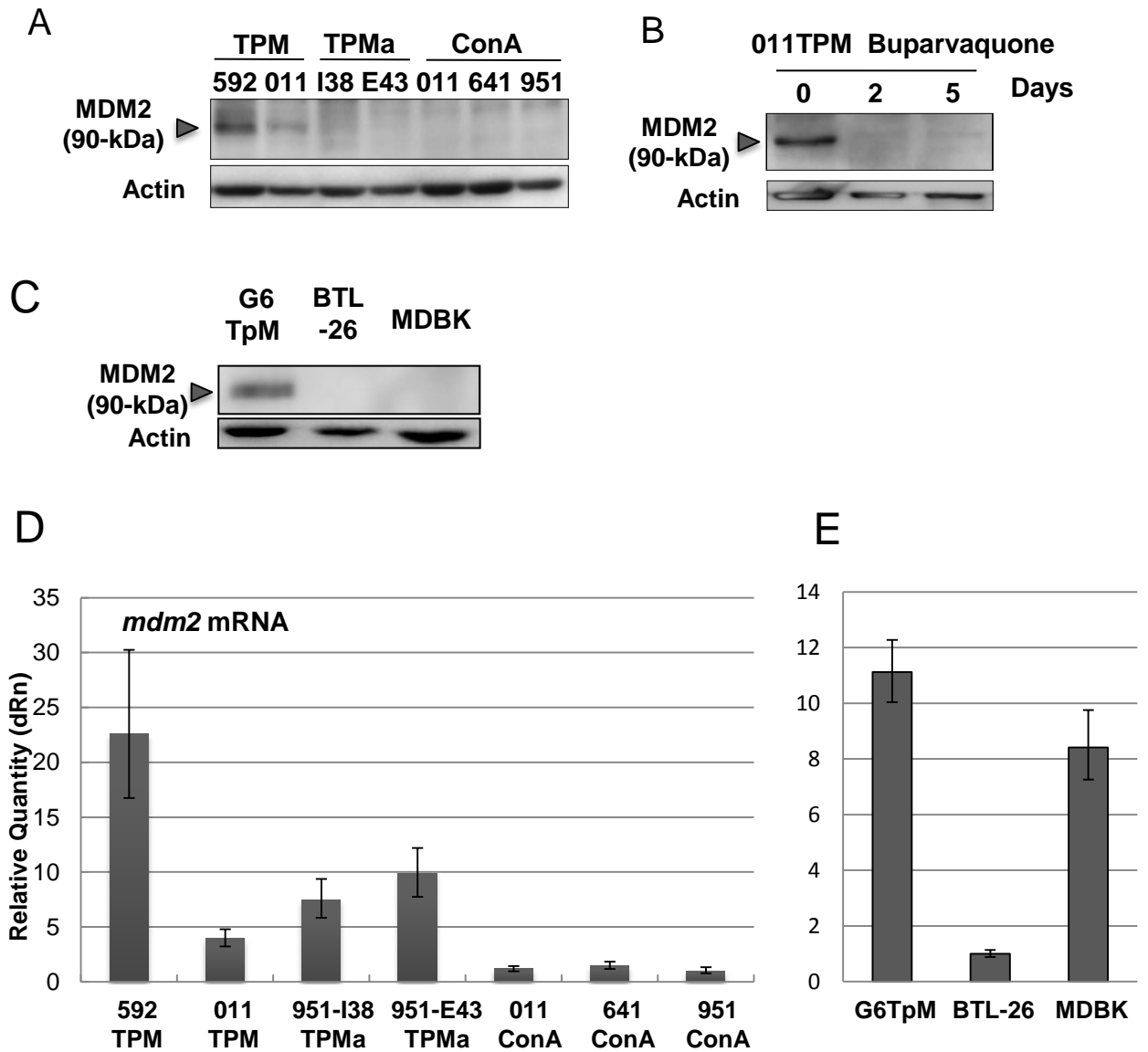
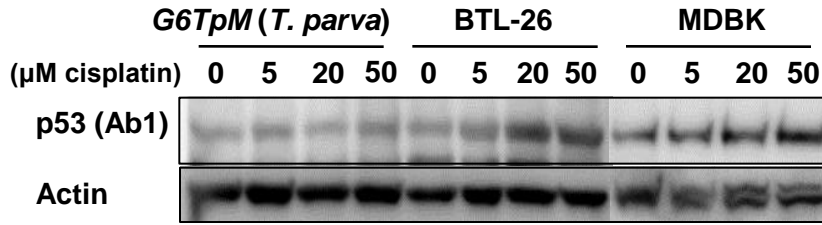
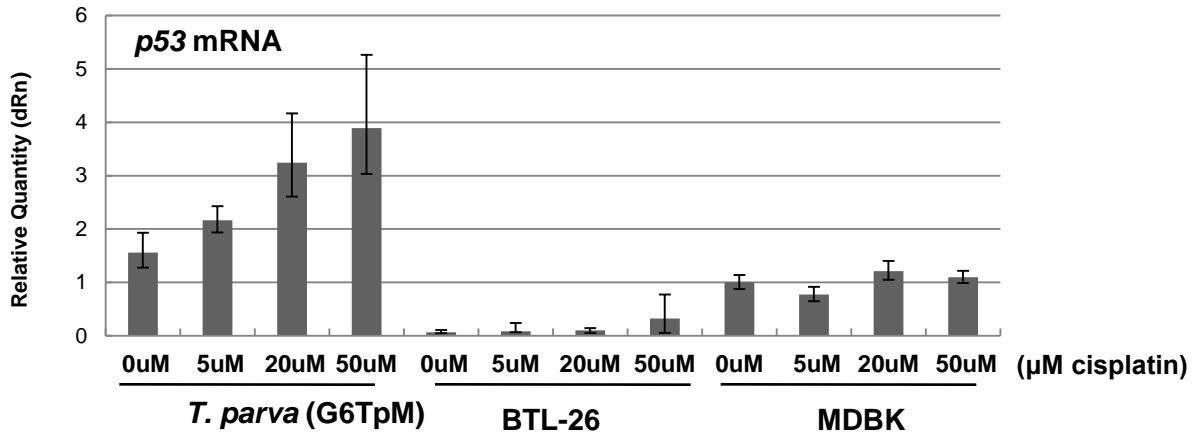


Figure 4

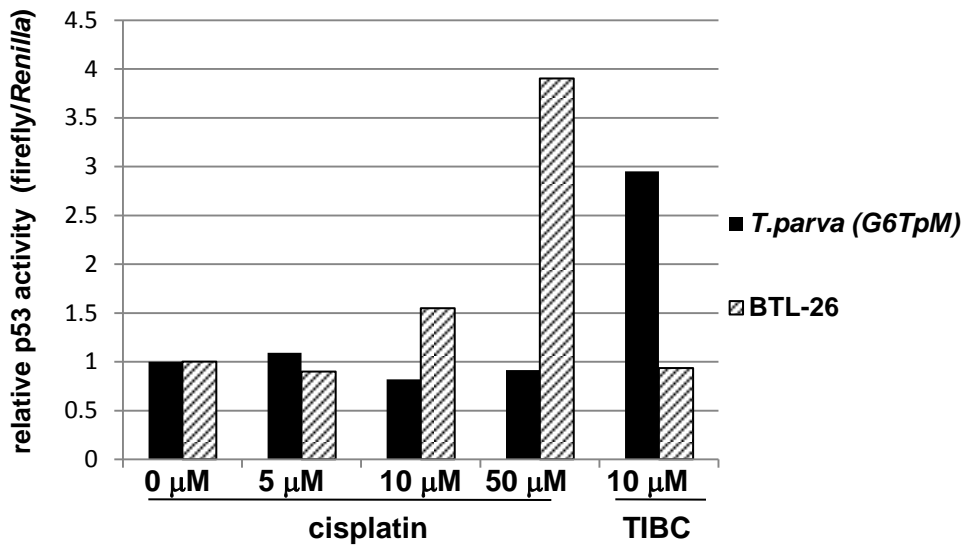
A



B



C



D

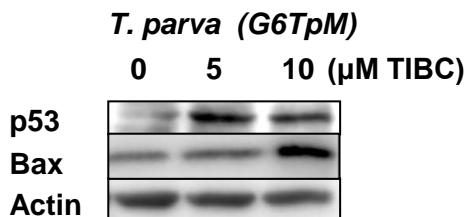


Figure 5

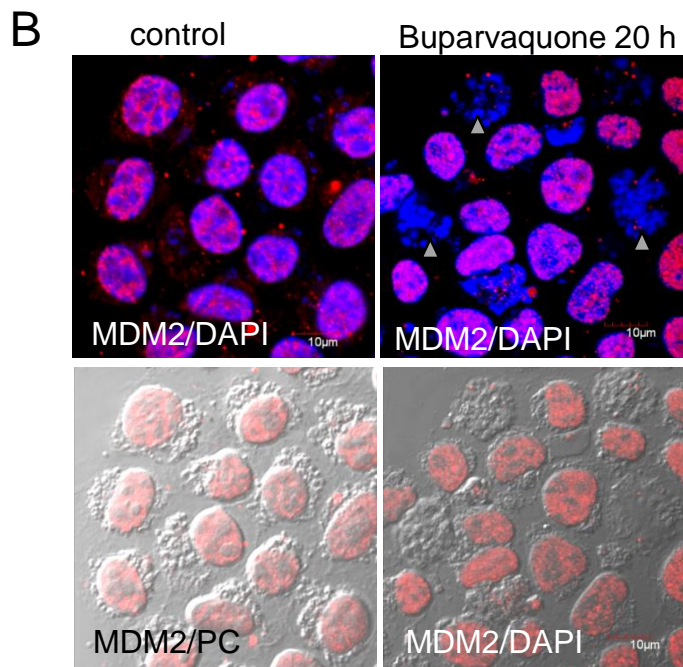
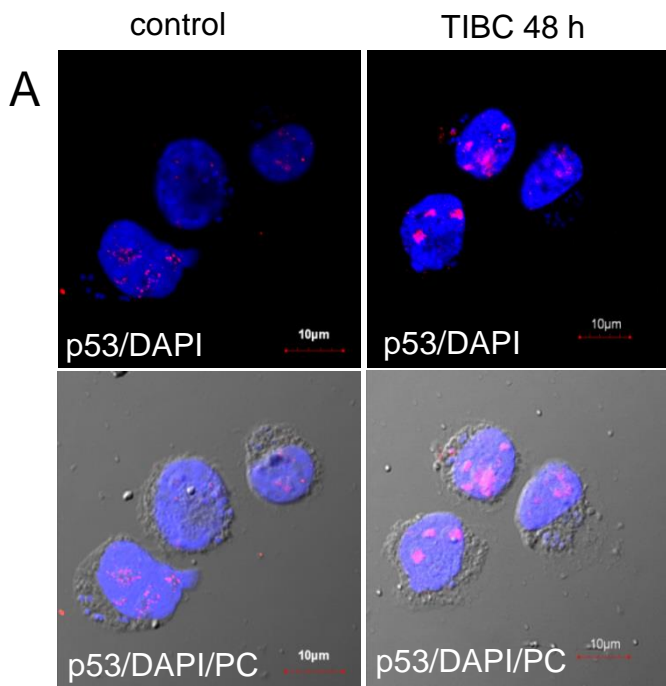


Figure 6

Table 1. A list of compounds that affect the proliferation of *T. parva*-infected lymphocytes.

	category	inhibitor	TP/ConA(%)
1	glucosidase I, II	Deoxynojirimycin	0.53
2	Jak-2	Cucurbitacin I	1.33
3	lipoxygenase	Nordihydroguaiaretic acid (NDGA)	1.44
4	guanylate cyclase	LY 83583	1.59
5	MPTP opener	Lonidamine	1.88
6	kinesin Eg5	Monastrol	2.36
7	guanylate cyclase	ODQ	2.62
8	fatty acid synthase (FAS)	C75	2.93
9	HAT	Anacardic acid	3.46
10	HIF	Chetomin	4.17
11	HIF-1a hydroxylase	Dimethyloxalylglycine	4.65
12	MPTP	Ro 5-4864	4.65
13	cathepsin B	CA-074	5.34
14	Bcr-Abl	AG957	6.60
15	farnesyltransferase	FTI-276	7.51
16	telomerase	b-Rubromycin	7.56
17	HER2 (erbB2/neu), EGFR	AG825	9.08
18	PKG	KT 5823	9.70
19	DAG kinase	R59022	11.18
20	MDM2	TIBC	12.05
21	FAS	Cerulenin	12.12
22	Ca-ATPase	Thapsigargin	14.71
23	Ca ionophore	Ionomycin	15.22
24	12-lipoxygenase	Baicalein	16.35
25	antitumor (topo I/II)	Aclarubicin	19.35
26	CDC2	Kenpaullone	19.83
27	CRM1	Leptomycin B (0.1mM)	20.00
28	myosin light chain kinase	ML-7	20.67
29	Na/K/Mg ATPase	Sanguinarine	21.05
30	EGFR	AG1478	21.39
31	kinesin Eg5	HR22C16	21.88
32	telomerase	MST-312	23.86
33	antitumor (DNA)	Doxorubicin, HCl	25.00
34	MDM2	Nutlin-3	26.52
35	cathepsin G	Z-GLF-CMK	26.92
36	antitumor (topo II)	Etoposide (VP-16)	28.57

T. parva-infected G6TpM cells and ConA-stimulated bovine lymphocytes were cultured with 10 μ M each of 190 inhibitors (SCADS inhibitor kits I and II) for 24 h, and cell proliferation rates were determined by BrdU-incorporation assay. The list shows 36 compounds that inhibited the proliferation of *T. parva*-infected lymphocytes by >90% compared with cells mock-treated with DMSO, and had specific inhibitory effects on *T. parva*-infected lymphocytes of <30% compared with ConA-stimulated lymphocytes, shown as TP/ConA (%) in this table.

Table2. A list of the cell lines used in this study.

abbreviated name	Parasite species and strain / summary of the cell lines	Host cell phenotype
G6TpM	<i>T. parva</i> Muguga stock	CD4-CD8+ T cell
592TPM	<i>T. parva</i> Muguga stock	B cell
011TPM	<i>T. parva</i> Muguga stock	T cell
951-I38TPMa	<i>T. parva</i> Marikebuni stock	CD4-CD8+T cell
951-E43TPMa	<i>T. parva</i> Marikebuni stock	CD4+ CD8- Tcell
BTL-26	bovine leukemia virus infected cell line	T cell
MDBK	Madin Darbey bovine kidney cell line	N.D.
011ConA 641ConA 951ConA	ConA stimulated PBMCs	N.D. (uncloned)

Eight *Theileria*-infected cell lines, including cells infected with *T. parva* Muguga, *T. parva* Marikebuni, and five non-infected cell lines were used in this study. Expression of surface markers was analyzed by flow cytometry following staining with bovine monoclonal antibodies directed against CD4 (ILA-12), CD8 (ILA-105), CD3 (MM1A), $\gamma\delta$ (GB21A), and IgM (IL-A30).